Int. Conf. on Jets, Wakes and Separated Flows, ICJWSF-2017
October 9-12, 2017, Cincinnati, Ohio USA

BI-STABLE STATES IN THE WAKE OF A SIMPLIFIED GROUND TRANSPORTATION SYSTEM (GTS) MODEL

*[1]A. Rao, [1]J. Zhang, [1]G. Minelli, [2]B. Basara and [1]S. Krajnović

[1]Vehicle Aerodynamics Laboratory (*VAL*), Department of Mechanics and Maritime Sciences, Chalmers University of Technology, Gothenburg 41296, Sweden.

[2]AVL List GmbH, Advanced Simulation Technologies, Hans-List-Platz 1, 8020 Graz, Austria.

anirudh.rao@chalmers.se

ABSTRACT

Recent experimental investigations of [1] in the wake of a Ground Transportation System (GTS) model has shown that the near wake topology is invariant over a large range of Reynolds numbers. A large eddy simulation (LES) is thus undertaken to investigate the flow topology in the near wake. In the vertical midplane behind the model, a flow state which is anti-symmetric to that reported in [1] is observed here, confirming the possibility of occurrence of bi-stable flow. Interestingly, the flow topology remains invariant to any increase in the gap height from the standard case, indicating that the underbody flow does not influence the bi-stable behaviour. Furthermore, the flow was also found to be insensitive to the incoming flow at a small yaw angle.

1 INTRODUCTION

The ground transportation system (GTS) model is a simplified cab-over-engine truck model and is representative of a tractor-trailer combination without any intermediate gap. The earliest experimental investigations of the GTS model by [2, 3] were performed with the aim of reducing drag by the use of several add-on devices such as slanted rear end and boat-tails to the base of the model (also see [4, 5, 6, 7, 8] and others). [3] reported a 19% reduction in the drag coefficient by the use of boat-tail plates. To accurately compare the flow features in the near wake with the experimental studies, several numerical investigations were performed by the use of computational fluid dynamics (CFD). [9, 10] obtained steady state solutions at $Re = 2 \times 10^6$ using using steady Reynolds-averaged Navier–Stokes (RANS) $k-\omega$ Menter model and Spalart-Allmaras model. They assessed the capability of these model by comparing the flow structures and surface pressure data obtained from the work of [3]. Behind the base of the model, two symmetrical vortices were observed in the numerical computations, while the experimental particle image velocimetry (PIV) data shows an asymmetrical vortex structure, with a bottom vortex closer to the base and the top vortex at a distance of a trailer-width downstream of the base. In the horizontal midplane, two symmetrical counter rotating vortices were captured in both the experiments and numerical simulations. While the numerical simulations did not accurately predict the pressure coefficient on the base, the prediction of the drag coefficient from the $k-\omega$ Menter model was in good agreement with the experiments.

[11] performed LES on a truncated GTS model, simulating the flow around the rear of the body which extends to a distance equal to the height of the model from the base. The simulations performed on a coarse and a fine meshes predicted the formation of an asymmetrical vortex structures in the near wake. The mean flow on both meshes predicted a large triangular vortex at the top and closer to the base, and the smaller vortex at the bottom further away from the base. They also observed the formation of two counter-rotating vortices from the top corners of the model which extend far downstream in the wake.

[12] performed numerical simulations using Detached Eddy Simulations (DES) and RNG $k-\varepsilon$ model at $Re = 2 \times 10^6$ for the GTS model. The DES captures the transient vortical structures and the shedding behind the body, the URANS predictions approached a steady state result. The resulting flow topology observed in their simulations are opposite to that observed in [1] and similar to the LES of [11]; although the vortex

structures observed are elongated in the streamwise direction. They further indicate that enough "upwash" was not generated to produce vortical structures similar to that of [3]. Nonetheless, the predicted drag coefficient from their URANS and DES were within 0.24% and 1.25% of the experimentally observed values, respectively. Numerical simulations were performed by [13] using body-fitted and immersed boundary grids to investigate the flow past a GTS. Using RANS $k-\varepsilon$ model, they predict the flow fields and the drag coefficient for the GTS. While symmetric vortices were observed in the vertical midplane, the two grids over-predicted the overall drag coefficient on the body.

More recently, [1] performed experimental investigations on a 1:40 scale GTS model in a water channel at $Re \simeq 2.7 \times 10^4$. The flow topology observed in the vertical midplane in [1] (see figure 1(c)) and [3] at $Re = 2 \times 10^6$ was similar, given the large disparity in Reynolds numbers. [1] also investigated the influence of the gap height on the wake topology. As the gap height between the ground and the model is increased from $0.03H$ to $0.14H$ (where H is the height of the GTS model), an asymmetrical flow topology was observed, with the size of the lower vortex increasing with gap height. However, for gap heights in excess of $0.14H$, the flow topology remained unaltered, with minimal change in the location of the centres of the vortices. The flow topology in the vertical midplane of the GTS predicted by numerical simulations of [11, 12] appear to be anti-symmetrical to that predicted by [1, 3]. The height-to-width ratio of the GTS model is 1.392, while the width-to-height ratio of the square-back Ahmed body is 1.35, indicating that bi-stable phenomenon could indeed be plausible in the vertical midplane of the GTS [1].

In this study, we use large eddy simulations (LES) to predict the near wake of a simplified GTS model at $Re \simeq 2.7 \times 10^4$ in order to compare directly with the experimental observations of [1]. The remainder of the article is organised as follows. Section 2.1 elucidates the problem setup, while section 2.2 briefly details the numerical method employed. The results from LES are presented in section 3, followed by conclusions in section 4.

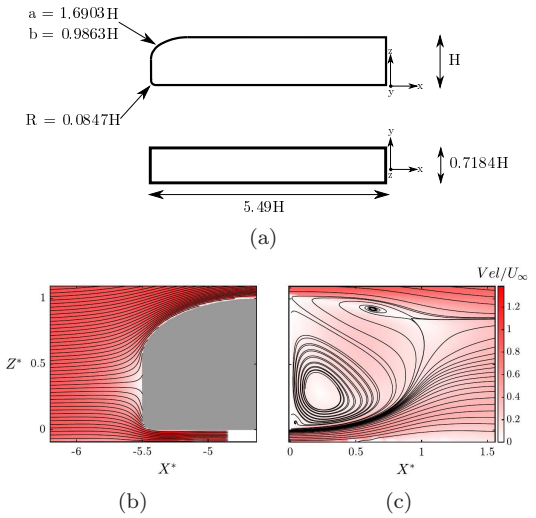

Figure 1: (a) Schematic of the GTS model showing the major dimensions of the model. The frontal shape of the model is elliptical, with the dimensions of the semi-major axis (a) and semi-minor axis (b) shown. Time-averaged flow at the (b) front and (c) rear of the GTS model in the vertical midplane reproduced from the experimental work of [1]. The abscissa and ordinate in (b) and (c) are normalised by the height of the model.

2 METHODOLOGY

2.1 PROBLEM SETUP

The GTS model is characteristic of a bluff body; with an elliptical front and an elongated section with a square back. The side and bottom edges at the front are curved, and is representative of a truck cabin with no gap to the trailer. In order to aid the construction of a purely hexahedral mesh, the curved A-pillars at the frontal sides of the model are removed, resulting in a sharp frontal edge along the side. This ensures a fixed separation point for the flow and may perhaps lead to a larger recirculation region compared to the experiments. The schematic of the GTS model used in this study is shown in figure 1(a) and the dimensions of the model are identical to that used by [3]. Two cases are considered in this study; one where the model is placed close to the ground at a height of $0.14H$, and the second case where the body is placed at a height of $1.1H$ above the ground, to study the influence of the shape of the model on the flow topology in the absence of ground effect.

The GTS model is placed at the centre of the computational domain, with the domain boundaries are placed at large distances from the model to ensure blockage less than $\simeq 1.5\%$. The inlet and outlet boundaries are at a distance of $18H$ and $25H$ from the origin, which is located at the bottom edge of the base of the model. The lateral and top boundaries extend $5H$ and $9H$ from the origin, respectively, and are assigned symmetry boundary conditions. The ground boundary condition used here is set to replicate the experimental work of [1], with a slip wall enclosing a no-

slip wall. The no-slip wall extends $2.5H$ and $7.5H$ upstream and downstream of the model, respectively, and $3H$ on either side of the model. While experimental investigations usually have cylindrical or streamlined supports, these were not used for the model considered here, thereby leading to unperturbed underbody flow. The inlet velocity was set to $U_\infty = 1.2768ms^{-1}$, leading to a $Re_W \simeq 2.7 \times 10^4$, where Re_W is the Reynolds number based on the width of the model.

The computational domain consisted purely of hexahedral elements, and three meshes were constructed to investigate the influence of the spatial resolution on the flow topology. For the GTS model at a gap height of $G = 0.14H$, the coarse, medium and fine meshes consisted of approximately 4.5, 8.5 and 11 million elements, respectively, and for the case where the GTS model is at a height of $1.1H$ above the ground, the mesh consisted of approximately 9 million elements, with a spatial resolution similar to the medium mesh. For all the cases considered here, the time-step used was set to $7.5 \times 10^{-3}s$ to ensure a CFL number less than unity around the GTS model. Averaging of the flow quantities and forces was carried out for five flow passages after initial transience of one flow passage.

2.2 NUMERICAL FORMULATION

The LES equations are discretised with a commercial finite volume solver, AVL FIRE, to solve the incompressible Navier—Stokes equations using a collocated grid arrangement. The algebraic eddy viscosity model originally proposed by Smagorinsky [14] is used in the present work for its simplicity and low computational cost. Convective fluxes are approximated by a blend of 95% central differences of second-order accuracy and of 5% upwind differences. The time integration is done using the second-order accurate three-level time Euler scheme. The numerical formulation has previously been validated for a wide range of bluff body investigations [15, 16, 17, 18, 19, 20, 21].

3 RESULTS

The flow past a simplified GTS model is investigated at $Re_W \simeq 2.7 \times 10^4$. Of interest here is the near wake in the vertical midplane where the flow topology of the time-averaged flow is anti-symmetric when compared to the studies of [1, 3] (see figure 1(c)). Shown in figures 2(a) - 2(c) are the time-averaged flow structures in the near wake obtained on the three meshes of increasing spatial resolution for the GTS model at a gap height of $0.14H$. The rear stagnation point is closer to the bottom edge of the model in the results of the coarse mesh, while for the medium mesh and the fine mesh, the location is slightly higher. The locations of the centres of the large triangular upper vortex and the smaller bottom vortex are within $5 - 10\%$ of that observed in the experiments (the reference point for measuring the distances is centred at the midpoint of the upper edge of the base of the model) for the three domains investigated. However, the saddle point was found to be further downstream as compared to the experiments. A tiny vortex is observed very close to the top of the base and this spans $\simeq 90\%$ of the width of the model. Also shown in figure 2(d) is the time-averaged flow when the model is placed at a height of $1.1H$ above the ground. The flow topology here is identical to that observed at $G/H = 0.14$, although the saddle point is located marginally downstream as compared to the other cases. Nonetheless, this validates the findings of [1], where the flow structures remained unaltered with gap height for $G/H \gtrsim 0.14$.

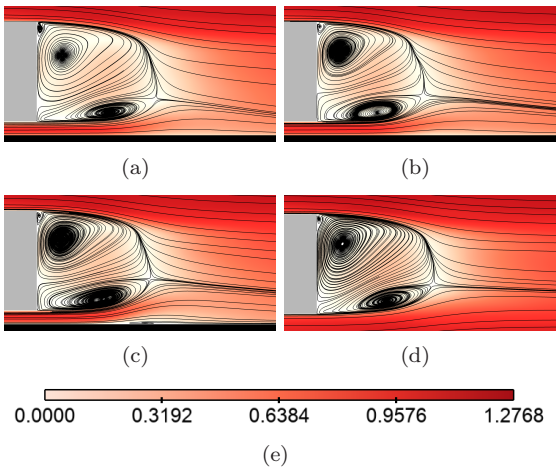

Figure 2: Visualisation of the contours of the time-averaged velocity overlaid with streamlines at the rear of the GTS model in the vertical midplane for the model at $G/H = 0.14$ for (a) coarse mesh, (b) medium mesh, (c) fine mesh, and (d) for a model at $G/H = 1.1$. Flow is from left to right in these images.

It may be recalled that bi-stability was observed in the lateral plane of a square-back Ahmed body, where the width-to-height ratio is approximately equal to the height-to width ratio of the GTS model [22, 23, 24, 25, 26, 27, 28, 29]. Thus, the flow structures observed here in the vertical midplane, and in the LES simulations of a truncated GTS model [11], are indeed one of the two flow states that can occur. The structure and location of the first few proper orthogonal decompo-

sition (POD) modes obtained in vertical midplane of the GTS is consistent with the modes observed in the lateral midplane of the square-back Ahmed body [1, 29]. Furthermore, given the relatively close match of the vortex locations in this study, the occurrence of the bi-stable flow phenomenon is demonstrated.

[22] reported the percentage of time the two bi-stables states was observed for a square-back Ahmed body. When the body was at a yaw angle of 0°, the ratio of the dominant larger triangular vortex on the left-to-right side was 28:72, and when yawed by 0.35°, the ratio was 90:10, indicating the sensitivity to the yaw angle. Here, the incoming flow was yawed by $\beta = 2.5°$ to investigate the occurrence the other bi-stable state. A flow topology similar to the non-yawed case was observed in the vertical midplane, indicating that this flow is insensitive to the incoming flow asymmetry. The GTS model is a slender-body, with its length being five times its height, and this could possibly explain the flow topology at the rear being insensitive to the incoming flow yaw angle and/or the absence of the curved A-pillars in this model.

Shown in figure 3(a) are the contours of the time-averaged flow at the front of the model in the vertical midplane. The stagnation point occurs at height of $\simeq 0.31H$ from the bottom edge of the model and the flow remains attached over the elliptical shaped nose, and beyond this region, a very small recirculation region is observed. This region is beyond the PIV window used in [1], who report that no separation occurred (see figure 1(b)). On the frontal sides of the model, the length of the recirculation zone is approximately $0.7H$, which is $0.2H$ longer than that reported in [1], due to the sharp edges in the current model. At the rear of the model, the two counter-rotating vortices are observed in the lateral midplane (figure 3(b)). The location of the centre of these vortices are $0.2H$ further downstream as compared to their experimental counterparts.

Shown in figure 4 are the isosurfaces of Q-criterion for the three meshes used. As the spatial resolution is increased, smaller scales structures are captured in the medium and fine meshes, as compared to the coarse mesh. These images further indicate that the flow is well resolved by the medium mesh.

The time-averaged forces experienced on the GTS models are detailed in table 1. The drag force coefficient experienced by the model with the medium mesh is within 1.6% of the fine mesh, while the lift coefficient is more sensitive to the increase in resolution. When the incoming flow is

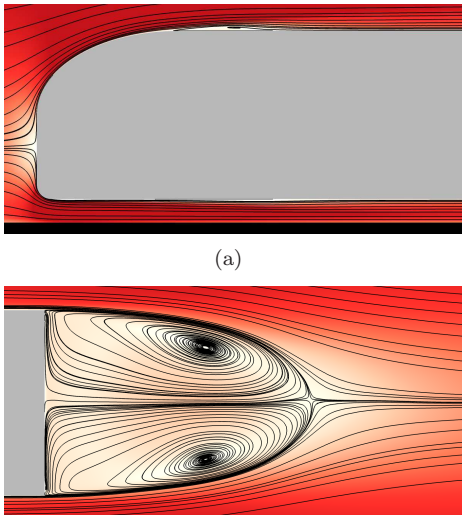

(a)

(b)

Figure 3: Visualisation of the contours of the time-averaged velocity overlaid with streamlines for the GTS model - medium mesh (a) in the vertical midplane at the front, and (b) in the lateral midplane at the rear. Flow is from left to right in these images. Contour shading as per figure 2.

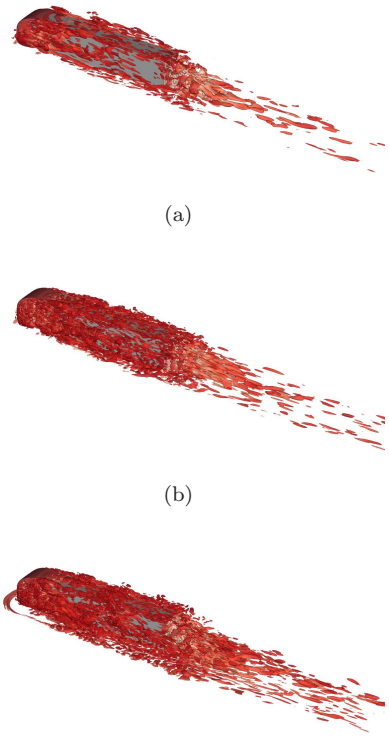

(a)

(b)

(c)

Figure 4: Isosurfaces of the Q-criterion ($= 10s^{-2}$) for (a) coarse mesh, (b) medium mesh and (c) fine mesh. Flow is from top left to bottom right in these images. Contour shading as per figure 2.

Table 1: Comparison of the time-averaged force coefficients on the GTS model for the various cases investigated in this study.

Description	$\overline{C_x}$	$\overline{C_y}$	$\overline{C_z}$
Coarse	0.5724	0.0029	-0.1885
Medium	0.5734	-0.0014	-0.2010
Fine	0.5658	-0.0027	-0.2153
$\beta = 2.5°$	0.5831	0.2948	-0.1810
$G/H = 1.1$	0.5776	-0.0009	-0.0588

yawed by $\beta = 2.5°$, an increase in the drag coefficient was observed along with a non-zero value of the sideways coefficient. As the gap height is increased from $0.14H$ to $1.1H$, the drag coefficient is similar to that of the medium mesh, further indicating that the observed flow topology is not significantly influenced by the underbody flow at a gap height of $0.14H$.

4 CONCLUSIONS

A LES study was undertaken to investigate the flow topology in the wake of a GTS model at a gap height of $G/D = 0.14$. A spatial resolution study was carried out on three grids, and in all cases, the flow topology in the vertical midplane was found to be anti-symmetric as compared to the experimental works of [1, 3]. The location of the vortex centres were in good agreement with their experimental counterparts, thereby confirming the occurrence of bi-stable flow. Furthermore, when the distance between the ground and the model was increased to $1.1H$, the flow topology remained unaltered, indicating that the gap height or the underbody flow does not play a significant role in determining the flow topology (and hence, the bi-stability). Furthermore, the topology in the near wake remains unaltered when the incoming flow velocity was yawed by 2.5°.

While the focus of the current study is primarily on the flow topology of the wake, a more detailed study is underway to explore the wake frequencies and POD modes, and if hybrid RANS-LES methods such as partially-averaged Navier–Stokes equations (PANS) can accurately predict the topology of the wake on coarser grids [20].

5 ACKNOWLEDGEMENTS

The authors would like to thank the computational support provided by Chalmers Centre for Computational Science and Engineering (C3SE) and National Supercomputer Centre (NSC) provided by the Swedish National Infrastructure for Computing (SNIC). The authors would also like to acknowledge the support and licences provided by AVL GmbH, Austria.

REFERENCES

[1] D. McArthur, D. Burton, M. C. Thompson, and J. Sheridan. On the near wake of a simplified heavy vehicle. *Journal of Fluids and Structures*, 66:293 – 314, 2016.

[2] R. H. Croll, W. T. Gutierrez, B. Hassan, J. E. Suazo, and A. J. Riggins. Experimental investigation of the ground transportation systems (GTS) project for heavy vehicle drag reduction. In *SAE Technical Paper*. SAE International, 1996.

[3] B.L. Storms, J.C. Ross, J.T. Heineck, S.M. Walker, D.M. Driver, and G.G. Zilliac. An experimental study of the ground transportation system (GTS) model in the NASA Ames 7-by 10-ft wind tunnel. *National Aeronautics and Space Administration, Ames Research Center*, pages 1 – 21, 2001.

[4] D. Burton, D. McArthur, J. Sheridan, and M. C. Thompson. Contribution of add-on components to the aerodynamic drag of a cab-over truck-trailer combination vehicle. *SAE Int. J. Commer. Veh.*, 6:477–485, 2013.

[5] J. J. Kim, S. Lee, M. Kim, D. You, and S. J. Lee. Salient drag reduction of a heavy vehicle using modified cab-roof fairings. *Journal of Wind Engineering and Industrial Aerodynamics*, 164:138 – 151, 2017.

[6] H. Martini, B. Bergqvist, L. Hjelm, and L. Löfdahl. Aerodynamic effects of roof deflector and cab side extenders for truck-trailer combinations. In *SAE Technical Paper*. SAE International, 2011.

[7] K. R. Cooper. Wind tunnel and track tests of class 8 tractors pulling single and tandem trailers fitted with side skirts and boat-tails. *SAE Int. J. Commer. Veh.*, 5:1–17, 2012.

[8] J. D. Coon and K. D. Visser. Drag reduction of a tractor-trailer using planar boat tail plates. In *The Aerodynamics of Heavy Vehicles: Trucks, Buses, and Trains*, pages 249–265. Springer Berlin Heidelberg, 2004.

[9] C. Roy, J. Payne, M. McWherter-Payne, and K. Salari. RANS simulations of a simplified tractor/trailer geometry. In *The Aerodynamics of Heavy Vehicles: Trucks, Buses, and*

Trains, pages 207–218. Springer Berlin Heidelberg, 2004.

[10] C. Roy, J. Payne, and M. McWherter-Payne. RANS simulations of a simplified tractor/trailer geometry. *Journal of Fluids Engineering*, 128(5):1083–1089, 2006.

[11] J. M. Ortega, T. Dunn, R. McCallen, and K. Salari. Computational simulation of a heavy vehicle trailer wake. In *The Aerodynamics of Heavy Vehicles: Trucks, Buses, and Trains*, pages 219–233. Springer Berlin Heidelberg, 2004.

[12] S. V. Unaune, S. D. Sovani, and S. E. Kim. Aerodynamics of a generic ground transportation system: Detached eddy simulation. In *SAE Technical Paper*. SAE International, 2005.

[13] R. Ghias, A. Khondge, and S. D. Sovani. Flow simulations around a generic ground transportation system: Using immersed boundary method. In *SAE Technical Paper*. SAE International, 2008.

[14] J. Smagorinsky. General Circulation Experiments with the Primitive Equations. *Monthly Weather Review*, 91:99, 1963.

[15] M. Mirzaei, S. Krajnović, and B. Basara. Partially-averaged Navier-Stokes simulations of flows around two different Ahmed bodies. *Computers and Fluids*, 117:273 – 286, 2015.

[16] J. Östh, B.R. Noack, S. Krajnović, D. Barros, and J. Borée. On the need for a nonlinear subscale turbulence term in pod models as exemplified for a high-Reynolds-number flow over an Ahmed body. *Journal of Fluid Mechanics*, 747:518544, 2014.

[17] J. Östh and S. Krajnović. A study of the aerodynamics of a generic container freight wagon using Large-Eddy Simulation. *Journal of Fluids and Structures*, 44:31 – 51, 2014.

[18] J. Östh, S. Krajnović, and B. Basara. LES study of breakdown control of A-pillar vortex. *International Journal of Flow Control*, 2(4):237–258, 2010.

[19] J. Östh and S. Krajnović. A LES study of a simplified tractor-trailer model. In *The Aerodynamics of Heavy Vehicles III*, pages 327–342. Springer, 2016.

[20] S. Krajnović, R. Lárusson, and B. Basara. Superiority of PANS compared to LES in predicting a rudimentary landing gear flow with affordable meshes. *International Journal of Heat and Fluid Flow*, 37:109–122, 2012.

[21] S. Krajnović and L. Davidson. Exploring the flow around a simplified bus with large eddy simulation and topological tools. In *The Aerodynamics of Heavy Vehicles: Trucks, Buses, and Trains*, pages 49–64. Springer Berlin Heidelberg, 2004.

[22] R. Volpe, P. Devinant, and A. Kourta. Unsteady experimental characterization of the natural wake of a squareback Ahmed model. Number 46230, pages V01CT17A007–1–V01CT17A007–7. ASME, 2014.

[23] R. Volpe, P. Devinant, and A. Kourta. Experimental characterization of the unsteady natural wake of the full-scale square back Ahmed body: flow bi-stability and spectral analysis. *Experiments in Fluids*, 56:99, 2015.

[24] A. Lahaye, A. Leroy, and A. Kourta. Aerodynamic characterisation of a square back bluff body flow. *International Journal of Aerodynamics*, 4(1-2):43–60, 2014.

[25] A. K. Perry, G. Pavia, and M. Passmore. Influence of short rear end tapers on the wake of a simplified square-back vehicle: wake topology and rear drag. *Experiments in Fluids*, 57(11):169, 2016.

[26] M. Grandemange, M. Gohlke, and O. Cadot. Turbulent wake past a three-dimensional blunt body. Part 1. Global modes and bi-stability. *Journal of Fluid Mechanics*, 722:5184, 2013.

[27] M. Grandemange, M. Gohlke, and O. Cadot. Turbulent wake past a three-dimensional blunt body. part 2. Experimental sensitivity analysis. *Journal of Fluid Mechanics*, 752:439–461, 2014.

[28] M. Grandemange, M. Gohlke, and O. Cadot. Bi-stability in the turbulent wake past parallelepiped bodies with various aspect ratios and wall effects. *Physics of Fluids*, 25(9):095103, 2013.

[29] A. Lahaye, A. Leroy, and A. Kourta. Characterisation of a square back Ahmed body nearwake flow. In *21 ème CongréS Français de mécanqiue, Bordeaux, France 26 - 30 August 2013*, 2013.